

# Control of the sound radiation of grid panels with active-passive-hybrid methods

By **M. Misol** AND **M. Titze** AND **H. P. Monner**

Institut für Faserverbundleichtbau und Adaptronik, Deutsches Zentrum für Luft- und Raumfahrt  
Lilienthalplatz 7, 38108, Braunschweig

The present work deals with the acoustic properties of grid-stiffened aircraft fuselage panels. It aims at the development of passive and active-passive-hybrid (APH) acoustic treatments to improve the low-frequency sound transmission loss of these grid panels. The idea is to exploit the geometric and dynamic properties of grid panels to improve the efficiency of the acoustic treatments. The work is subdivided in several tasks. It starts with the definition and manufacturing of an aircraft relevant test specimen. A laboratory setup is build in a semi-anechoic room which permits a proper mounting, excitation and measurement of the grid panel. A finite element model of the panel is developed and validated by means of experimental modal analysis. An aircraft relevant load case is defined and implemented. For this, a synthesis of the structural vibration induced by a turbulent boundary layer is realized by using a number of loudspeakers. Based on this work, the passive and APH acoustic treatments will be developed and implemented in the sequel of the project.

---

## 1. Introduction

One topic of the Sonderforschungsbereich 880 is the prediction and the abatement of cabin noise associated with novel aircraft engines like ultra-high-bypass-ratio (UHBR) engines. The fuselage structure is crucial for sound transmission and hence its configuration will heavily influence the noise level in the cabin. The conventional setup is a double panel system consisting of the fuselage structure and a trim panel. This setup provides high transmission loss at mid and high frequencies. Alternative fuselage designs with sandwich or grid panels have different sound transmission properties and might require or facilitate other noise control methods. The low coincidence frequencies of novel lightweight fuselage structures in combination with UHBR or counter-rotating-open-rotor (CROR) engines might lead to increased noise levels in the cabin. Therefore, in this work, the vibro-acoustic behavior of a grid-stiffened panel structure is investigated and passive and active-passive-hybrid (APH) noise control techniques are applied.

Research on grid-stiffened structures has a long history in rocket science (e. g. CRISM in the 1980s) [1]. More recent research projects also consider grid-stiffened aircraft fuselage structures [2]. Most of these projects focus on weight and cost reduction issues and do not take into account the vibro-acoustic behavior and sound transmission properties of grid structures. Some activities related to the passive damping of grid structures and the implications on sound transmission are published by Drake et al. [3]. The application of APH methods to grid panels is basically unexplored. Therefore, a patent application

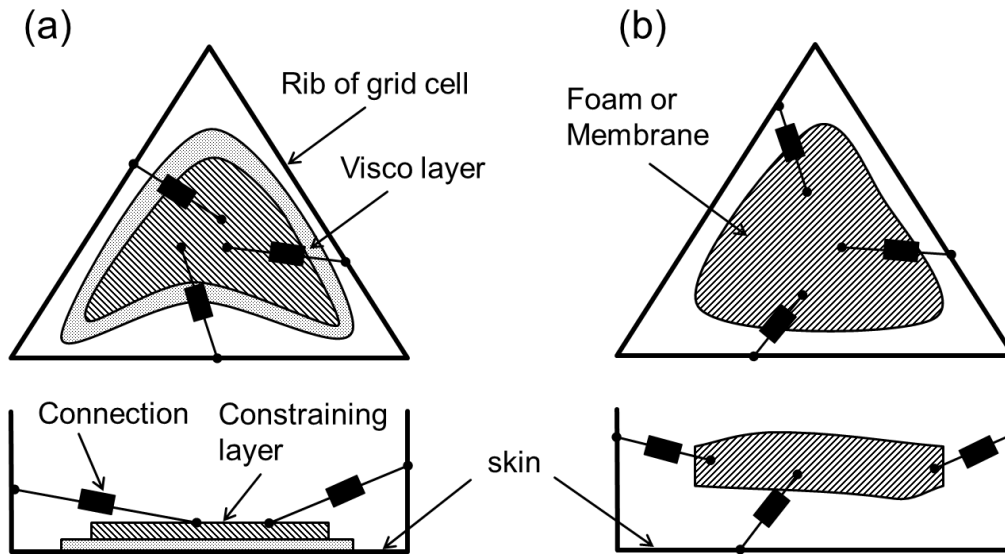


FIGURE 1. The general idea of applying APH methods to grid panels.

was submitted by the author to claim this new idea [4].

Well-known APH methods are the active constrained layer damping [5], smart foams [6,7], active tiles [8,9] or active skins [10]. These methods have been applied to conventional panel and fuselage structure but not to grid panels. The basic idea of this project is to make use of the specific geometric and dynamic characteristics of grid panels for the efficient implementation of APH methods. The main objectives are to set up a validated simulation model of a grid panel, to realize a laboratory setup with a grid panel, to implement selected APH methods and to evaluate their acoustic performance in the acoustic laboratory.

## 2. Approach

The application of APH methods to grid panels for the reduction of sound emission is the central issue of this project. Figure 1 visualizes the general idea of this approach. A grid panel is made up of a skin stiffened by different ribs (cp. Fig. 2). A skin field enclosed by these ribs forms a grid cell. These cells must not be identical and may have different shapes. In Fig. 1 a generic triangular cell is shown which is augmented by structural damping (a) or acoustic damping (b). One example for structural damping is passive or active constrained layer damping. Constrained layer damping combines a visco layer with a passive or active constraining layer to maximize the strain in the visco layer. One special characteristic is the connection of the constraining layer to the ribs of the grid cell via a passive or active structural link. Acoustic damping or radiation impedance control can be achieved with passive or active foams (smart foams) or membranes. This principle is visualized in Fig. 1 (b). Here as well, a structural link between the ribs and/or the skin is intended. More details can be found in the patent application of Misol [4].

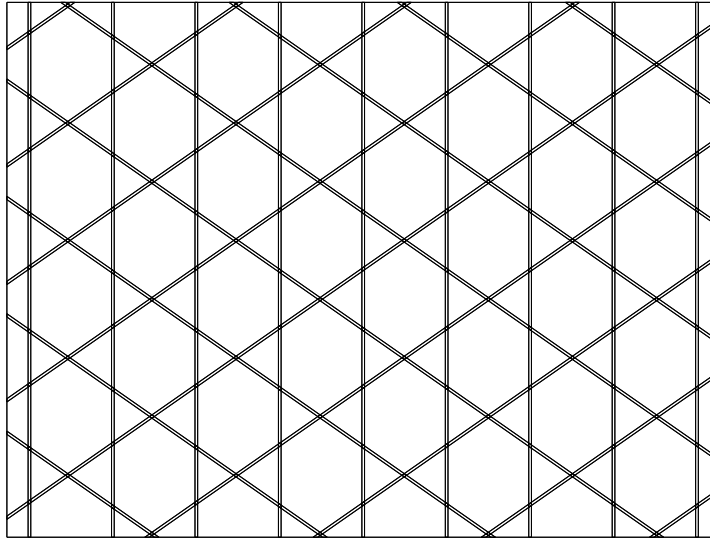


FIGURE 2. Geometry of the grid panel test specimen.

The project is subdivided into the following main tasks:

- definition of the test specimen
- definition of the laboratory setup
- modeling, simulation and validation
- definition of the load case
- implementation of passive methods
- implementation of active-passive-hybrid methods

The main project work started in the end of 2016 and hence the reporting period is approx. six months. In this period the first four items have been accomplished. The implementation of passive and APH methods is the subject of future work. Therefore, in this report, no further details and results can be provided regarding the last two items.

The project starts with the definition of a test specimen. The size of the structure is mainly limited by laboratory and monetary restrictions. For budgetary reasons, a flat panel is fabricated in aluminum instead of carbon fibre reinforced plastics (CFRP). It is assumed that these simplifications will not imply a loss of generality of the obtained results. The geometric properties of the grid panel are listed in Tab. 1. They are adopted from Vasiliev et al. [11, p. 65]. Figure 2 shows the final design of the test specimen with the vertical hoop ribs and the helical ribs inclined with a positive or negative angle from the horizontal. The grid panel is not made of a solid aluminum block but from a skin and individual ribs which are laser cut at the intersection points. For assembly the ribs are stucked together and glued at the intersection points and at the skin contact area by means of the structural glue ADEKIT A 170 BK. As will be discussed later, this manufacturing method induced significant complications for modeling and validation because a monolithic treatment (as if the structure was milled from one part) turned out to be infeasible.

rib height	30 mm
rib thickness	3 mm
separation of helical ribs	108 mm
separation of hoop ribs	93.6 mm
angle between helical and hoop ribs	55 deg
skin thickness	1.5 mm
panel width	800 mm
panel height	600 mm
panel mass	5.125 kg

TABLE 1. Geometric properties of the grid panel test specimen.

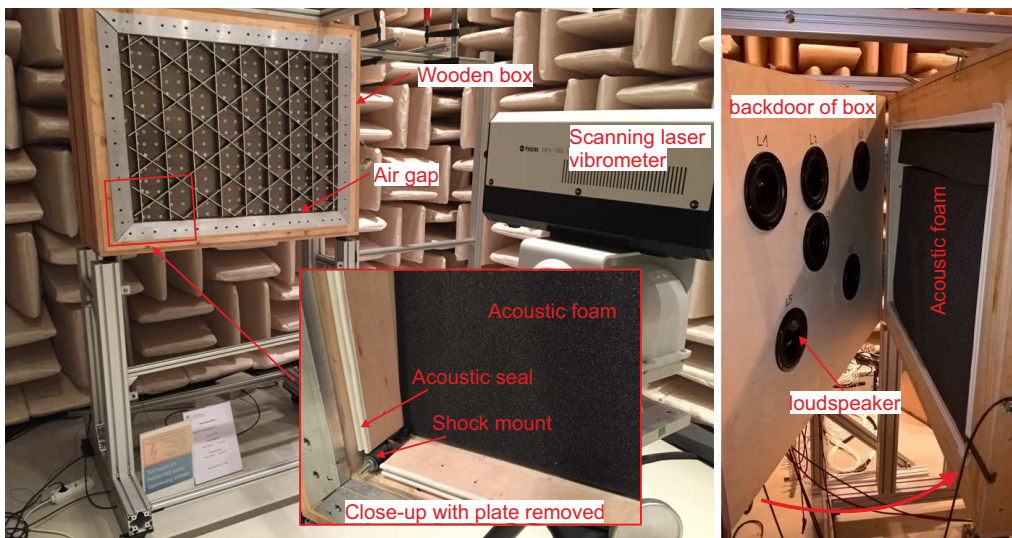


FIGURE 3. Laboratory setup in the semi-anechoic room of the transmission loss facility.

The laboratory setup is shown in Fig. 3. The grid panel is mounted in a wooden box by means of four shock mounts (Schwingmetall type A, 55 Shore) located at the corners (see close-up in Fig. 3). The shock mounts are chosen stiff enough to prevent substantial deepening of the panel and soft enough to keep the eigenfrequencies of the rigid body modes well below the eigenfrequencies of the flexural modes (87.8% isolation degree at 100 Hz). To preserve an air space around the plate edges, the panel dimensions are chosen slightly smaller than the clear opening of the wooden box. This permits relatively well defined boundary conditions for the simulation model. For experimental modal analysis, the panel was excited by one or two electrodynamic exciters (shaker) at defined positions (not shown). The final load case is realized by means of the six loudspeakers mounted at the backdoor of the wooden box (cp. Fig. 3). This facilitates more realistic structural excitation compared to the discrete force excitation of a shaker. The use of loudspeakers, however, requires additional sound proofing to minimize cavity resonances and sound leakage through the air gaps. As shown in Fig. 3, acoustic foam and seals are used to achieve this goal. A scanning laser vibrometer is used to measure the normal surface velocity of the grid panel.

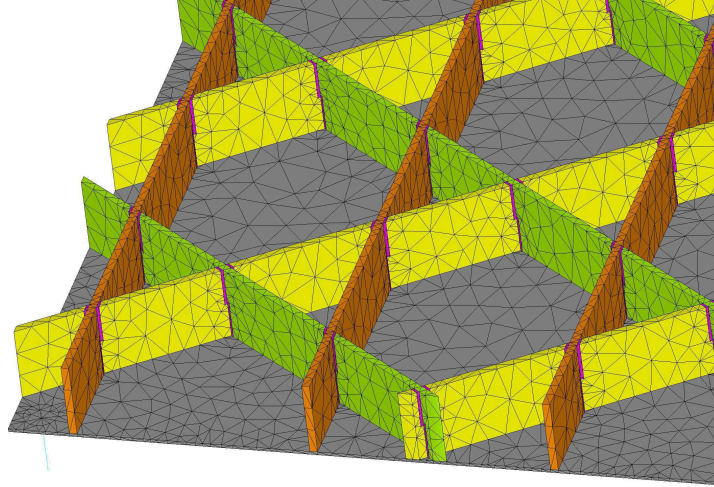


FIGURE 4. Detail of the FE model of the grid panel.

A finite-element (FE) simulation model was developed (Ansys Workbench) based on the definition of the test specimen and the laboratory setup. Initially, a simple monolithic approach was followed neglecting the effects of the imperfect rib intersections and the glue (assumption of a milled aluminium block). It turned out from experimental modal analysis, that these simplifications are not permissible, since they have a significant influence on the eigenproperties of the structure. Figure 4 shows the final configuration of the FE model with the skin in grey, the three rib types in orange, yellow and green and the adhesive surface areas in purple. The shock mounts are modeled with Ansys COMBIN14 elements. The skin and the ribs are modeled as aluminum using typical values for Youngs modulus and mass density. Likewise the adhesive ADEKIT is defined by these two parameters. The model updating was done with the help of optiSLang (Dynardo) which uses sensitivity analyses and different optimization algorithms. Optimization parameters are the two Youngs moduli, the two mass densities and the spring stiffness of the COMBIN14 elements. The performance metric for the optimization of these parameters is defined according to Eq. 2.1 with  $N = 10$ .

$$\min \left( \left( \left( \sum_{n=1}^N \frac{|f_{FEM,n} - f_{EMA,n}|}{f_{EMA,n}} \right) \cdot \frac{1}{N} + \left( \sum_{n=1}^N |MAC_n - 1| \right) \cdot \frac{1}{N} \right) \cdot \frac{1}{2} \right) \quad (2.1)$$

The damping optimization is done in a subsequent step by minimizing the deviation of the simulated and measures amplitudes of the normal surface velocities of the panel. The final results of the optimization will be discussed in Section 3.

An aircraft relevant load case must be defined to implement and evaluate the passive and APH acoustic treatments. One of the most important external source for aircraft interior noise is the turbulent boundary layer (TBL) [12]. Therefore, acoustic treatments derived for a TBL load case are meaningful for most aircraft configurations. Furthermore, the TBL is not selective concerning the excitation of the structural modes. This increases the relevance of the results.

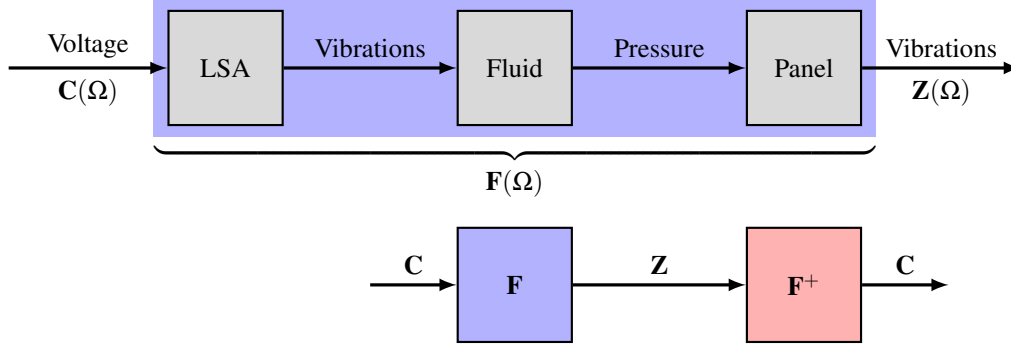


FIGURE 5. Block diagram of the laboratory TBL vibration field synthesis process.

The pressure field in a fully developed TBL can be statistically described by the so-called Corcos model [13]. According to the Corcos model, the cross-power spectral density (CPSD) of two pressure signals  $x$  and  $y$  measured in a fully developed TBL is given by

$$S_{xy}(\omega) = S_{xx}(\omega) e^{-|r_{sp}|/L_{sp}(\omega)} e^{-|r_{st}|/L_{st}(\omega)} e^{-j\omega r_{st}/U_c}. \quad (2.2)$$

In this formula  $S_{xx}$  describes the power spectral density (PSD) of  $x$  which is assumed to be identical at any point in the TBL pressure field. This is true when the TBL grows slowly and when the TBL pressure field is homogenous. The distances between two points in the span- and streamwise directions are  $r_{sp}$  and  $r_{st}$  and the corresponding correlation lengths are  $L_{sp}$  and  $L_{st}$ .  $U_c$  is the convection velocity which is assumed  $135 \text{ m/s}$  (corresponds to Mach  $\approx 0.66$ ). The correlation lengths are defined as  $L_{sp/st} = \alpha_{sp/st} U_c / \omega$  and the  $\alpha$ -values are defined as  $\alpha_{sp} = 1.2$  and  $\alpha_{st} = 8$ . The numerical values for the TBL parameters are adopted from Elliott et al. [14]. The PSD was measured in the Acoustic Wind-Tunnel Braunschweig (AWB) [15]. A regular FE grid with 1271 nodes is derived for the skin field of the grid panel. The CPSD is evaluated for all combinations of nodes of this FE grid and the corresponding 1271 nodal force spectra are derived. These force spectra are used as input data (structural excitation) for the numerical harmonic analysis of the grid panel. The result of this simulation is a vector of target normal surface velocity spectra  $\mathbf{Z}$  (cp. Fig. 5) which can be emulated by means of the loudspeakers of the wooden box (LSA). The speaker control voltages  $\mathbf{C}$  are obtained from filtering  $\mathbf{Z}$  through the pseudoinverse  $\mathbf{F}^+$  of the frequency response function matrix  $\mathbf{F}$  from the loudspeaker control voltages to the normal surface velocities of the panel. An overview of this process is shown in Fig. 5 in a block diagram form. The results of the vibration field synthesis (which implements the load case) will be provided in Section 3.

### 3. Results

Since the acoustic treatments are not implemented yet, results are provided for the modeling and the load case implementation only. Table 2 compares the eigenfrequencies from experimental modal analysis (EMA, done with software x-modal III) and the eigenfrequencies from numerical modal analysis (FEM) for the first ten modes. Furthermore, the modal assurance criterion (MAC) is provided which quantifies the consistency of measured and simulated mode shapes. It can be seen, that even after optimization of the structural parameters some deviations between EMA and FEM remain. This is

	EMA (Hz)	FEM (Hz)	MAC
Mode 1	37,15	32,79	0,995
Mode 2	61,02	56,75	0,961
Mode 3	71,26	61,51	0,948
Mode 4	152,74	151,51	0,963
Mode 5	168,19	165,53	0,972
Mode 6	296,51	301,48	0,995
Mode 7	360,67	360,62	0,992
Mode 8	381,86	377,23	0,995
Mode 9	457,52	480,93	0,921
Mode 10	466,84	484,14	0,897

TABLE 2. Measured (EMA) and simulated (FEM) Eigenfrequencies and MAC values of the grid panel. Only the flexural modes 4 to 10 are optimized.

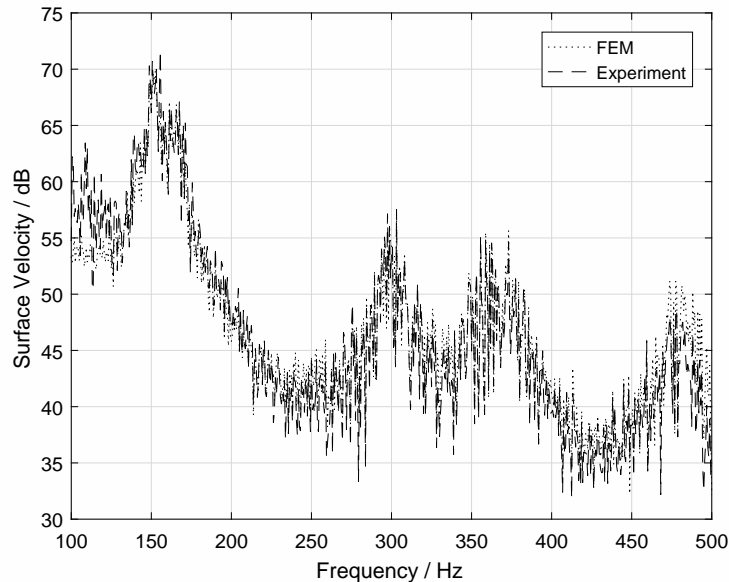


FIGURE 6. Comparison of simulated and measured average normal surface velocity of the grid panel for the TBL load case.

mainly attributed to the glued connections at the intersection points because each connection is slightly different (e. g. variation of adhesive layer thickness). A comparison of the simulated and measured radiated sound power will show, if the deviations are tolerable.

Figure 6 provides a comparison between the simulated (FEM) and measured average surface velocity in the frequency range containing modes 4 to 10 (the first seven flexural modes). It can be seen that the target vibration spectra from simulation (prescribed by the load case) are closely matched. This load case can be used for the implementation and evaluation of the passive and APH acoustic treatments.

#### 4. Conclusions

The application of APH methods to grid panels for the reduction of sound emission is the central issue of this project. In the reporting period, preliminary work was done for the implementation and evaluation of passive and APH acoustic treatments. An aircraft relevant test structure was defined and manufactured, a laboratory setup in a semi-anechoic room was build and vibro-acoustic measurement was done. A validated FE simulation model of a grid panel was derived, a aircraft relevant load case was defined and implemented. Based on this work, the passive and APH acoustic treatments will be realized in the sequel of the project.

#### Acknowledgments

Financial support has been provided by the German Research Foundation (Deutsche Forschungsgemeinschaft – DFG) in the framework of the Sonderforschungsbereich 880.

#### References

#### References

- [1] VASILIEV, V. V., BARYNIN, V. A. AND RASIN, A. F. (2001). Anisogrid lattice structures – survey of development and application. *Composite Structures*, **54**(2–3), 361–370.
- [2] NIEMANN, S., KOLESNIKOV, B., LOHSE-BUSCH, H., HÜHNE, QUERIN, O. M., TOROPOV, V. V. AND LIU, D. (2013). The use of topology optimisation in the conceptual design of next generation lattice composite aircraft fuselage structures. *Aeronautical Journal*, **117**(1197), 1139–1154.
- [3] DRAKE, M. L., KOURY, J. L., KIM, T. D. AND HARVEY, J. A. (1993). Integral acoustic control system for composite isogrid structures. *SPIE Vol. 1917 Smart Structures and Intelligent Systems*, **1917**, 623–633.
- [4] MISOL, M. (2016) *Wand mit einer durch rückwärtige Stege in Gitterfelder unterteilten Außenhaut und Flugobjekt*. Patent DE 10 2016 115 994.8.
- [5] AKL, W. AND BAZ, A. (2006) Active vibration and noise control using smart foam. *Journal of Vibration and Control*, **12**(11), 1173–1203.
- [6] GENTRY, C. A., GUIGOU, C. AND FULLER, C. R. (1997) Smart foam for applications in passive-active noise radiation control. *The Journal of the Acoustical Society of America*, **101**(4), 1771–1778.
- [7] GUIGOU, C. AND FULLER, C. R. (1999) Control of aircraft interior broadband noise with foam-pvdf smart skin. *Journal of Sound and Vibration*, **220**(3), 541–557.
- [8] JOHNSON, M. E. AND ELLIOTT, S. J. (1997) Active control of sound radiation from vibrating surfaces using arrays of discrete actuators. *Journal of Sound and Vibration*, **207**(5), 743–759.
- [9] GOLDSTEIN, A. (2006) *Control of sound transmission with active-passive tiles*. Ph.D. thesis, Virginia Polytechnic Institute and State University, Blacksburg, VA, USA.
- [10] JOHNSON, B. D. AND FULLER, C. R. (2000) Broadband control of plate radiation using a piezoelectric, double-amplifier active-skin and structural acoustic sensing. *The Journal of the Acoustical Society of America*, **107**(2), 876–884

- [11] VASILIEV, V. V. AND NIKITYUK, V. (2014) Development of geodesic composite fuselage structure. *International Review of Aerospace Engineering (IREASE)*, **7**(2), 61–68.
- [12] MIXSON, J. S. AND WILBY, J. F. (1991) Aeroacoustics of Flight Vehicles: Theory and Practice. *NASA Langley Research Center*, **2**(16), 271–355.
- [13] CORCOS, G. M. (1963) Resolution of pressure in turbulence. *The Journal of the Acoustical Society of America*, **35**(2), 192–199.
- [14] ELLIOTT, S. J., MAURY, C. AND GARDONIO, P. (2005) The synthesis of spatially correlated random pressure fields. *The Journal of the Acoustical Society of America*, **117**(3), 1186–1201.
- [15] HU, N. AND MISOL, M. (2015) Effects of riblet surfaces on boundary-layer-induced surface pressure fluctuations and surface vibration. In: *Proceedings of 41st Deutsche Jahrestagung für Akustik (DAGA)*, Nürnberg, Germany.